PAPER

Check for updates

Real time monitoring of biofilm formation on coated medical devices for the reduction and interception of bacterial infections†

Yasin Kurmoo, [ID] [a] Andrew L. Hook, [ID] [a] Daniel Harvey,[b] Jean-Frédéric Dubern, [ID] [c] Paul Williams, [ID] [c] Stephen P. Morgan, [ID] [d] Serhiy Korposh [ID] [d] and Morgan R. Alexander [ID] *[a]

Real time monitoring of bacterial attachment to medical devices provides opportunities to detect early biofilm formation and instigate appropriate interventions before infection develops. This study utilises long period grating (LPG) optical fibre sensors, incorporated into the lumen of endotracheal tubes (ETTs), to monitor in real time, *Pseudomonas aeruginosa* surface colonisation and biofilm formation. The wavelength shift of LPG attenuation bands was monitored for 24 h and compared with biofilm biomass, quantified using confocal fluorescence microscopy imaging. Biofilm formation was compared on uncoated ETTs and optical fibres, and on a biofilm resistant acrylate polymer, after challenge in an artificial sputum or minimal growth medium (RPMI-1640). The LPG sensor was able to detect a biofilm biomass as low as 81 μg cm^{-2}, by comparison with the confocal image quantification. An empirical exponential function was found to link the optical attenuation wavelength shift with the inverse of the biofilm biomass, allowing quantification of biofouling from the spectral response. Quantification from the sensor allows infection interception and early device removal, to reduce, for example, the risk of ventilator associated pneumonia.

Introduction

Bacterial attachment and subsequent biofilm formation on medical device surfaces is a prerequisite for device-centred infections.[1] Biofilms are aggregates of bacterial cells, encased in a slime layer, incorporating extracellular polymeric substances (EPS).[2] Produced by bacteria, EPS contains exopolysaccharides, extracellular DNA, proteins and other components, which provide environmental protection and restrict access of antimicrobials to the cells.[3] Bacteria within biofilms are up to 1000 times more tolerant to antimicrobials and the host immune system than planktonic cells, and are able to develop antimicrobial resistance through the exchange of resistance genes.[4,5] The general biofilm life cycle for pathogens such as *Pseudomonas aeruginosa* has been described as a five-step process; (1) reversible attachment, (2) irreversible attachment, (3) early maturation, (4) late maturation and (5) dispersal.[6] Pathogenic bacteria undergoing this life cycle on medical device surfaces pose a major infection risk to patients with indwelling devices.[1]

P. aeruginosa is a human pathogen capable of causing device-associated infections *via* biofilm formation.[7] An opportunistic, Gram-negative bacterium, it produces multiple virulence factors and a dense EPS layer containing up to three different exopolysaccharides (alginate, Pel and Psl).[8] This provides an effective barrier against host defences, making biofilms difficult to treat and eradicate, especially as they also release and disperse bacterial cells to colonise new sites throughout the host. *P. aeruginosa* colonisation of medical devices facilitates secondary nosocomial infections; biofilms on central venous catheters and endotracheal tubes (ETTs) can cause severe blood-borne infections and ventilator associated pneumonia (VAP) respectively.[9–11] These infections are major causes of morbidity and mortality in healthcare settings and impose significant economic costs. For example, cases of VAP alone are associated with up to 40 000 deaths in the United States annually and can cost up to USD 40 000 to treat per infection.[12,13]

In attempting to reduce device associated-infections, a number of modifications have been implemented. Antimicrobials such as antibiotics and silver have been incor-

[a]*School of Pharmacy, Boots Science Building, University Park, Nottingham, NG7 2RD, UK. E-mail: morgan.alexander@nottingham.ac.uk*
[b]*Department of Anaesthesia and Critical Care, School of Medicine, University Park, Nottingham, NG7 2RD, UK*
[c]*Centre for Biomolecular Sciences, University Park, Nottingham, NG7 2RD, UK*
[d]*Optics and Photonics Research Group, Faculty of Engineering, University Park, Nottingham, NG7 2RD, UK*
†Electronic supplementary information (ESI) available. See DOI: 10.1039/c9bm00875f

porated as a strategy to kill surface attached bacteria and biofilms.[14–16] Silver-embedded devices have shown a small but statistically significant reduction in the rate of infection associated with ETTs, although this result has not been replicated for other devices such as urinary catheters.[14,15] An alternative approach is the creation of anti-fouling coatings such as poly (ethylene glycol)[17] or zwitterionic based polymer coatings.[18] Recently, we reported a new class of amphiphilic polymers resistant to biofilm formation that achieved two orders of magnitude reduction in bacterial numbers within a murine subcutaneous infection model.[19] A reduction in biofilm formation was demonstrated on these polymers for the bacterial species *P. aeruginosa*, *Staphylococcus aureus* and *Escherichia coli* in a urinary catheter context[19,20] which may be relevant for preventing infections on ETTs. This reduction in biofilm formation is attributed to the chemical structure of the pendant groups of the polymer. The exact mechanism has not been fully established, although Sanni *et al.* has determined a relationship between resistant polymer pendant structures and *P. aeruginosa* attachment.[59] The amphiphilic copolymer has been CE-marked for use in humans as a urinary catheter coating, which is returning positive preliminary clinical trial results,[60] and is an inexpensive polymer that could readily be used to coat ETTs and other medical devices for the prevention of biofilm formation *in situ*.

Monitoring real time biofilm formation of pathogens such as *P. aeruginosa* to biomedical devices in the clinic would enable immediate action to be taken when the initial stages of bacterial attachment were detected, such as prompt antibiotic treatment or device removal. This would prevent biofilm maturation and mitigate secondary problems associated with biofilms and chronic infections. Early intervention can prevent biofilms progressing to the dispersion phase of the life cycle, from which systemic infection can ensue.[21] In addition to individual health benefits, this approach would reduce the costs associated with patient treatment. Currently, device-related infections are diagnosed through patient symptoms, with further analysis of the developed biofilm requiring removal of the device for microbiological and microscopic examination. This time consuming process delays the necessary remedial action from being taken to prevent an infection from worsening. In the case of ETTs, repeated removal and reinsertion of devices causes tracheal wall injury and facilitates VAP.[22,23] Surface plasmon resonance imaging (SPRi) has also been used experimentally for label free monitoring of biofilm formation on surfaces in real time[24,25] as have a variety of other optical techniques.[61] Although highly sensitive, these techniques still require device removal, are time consuming and necessitate multiple components, which incur high costs. Alternatively, non-invasive *in vivo* optical detection of biofilms in the human middle ear has been achieved using optical coherence tomography (OCT).[62]

Here, we report the use of optical fibre sensors for monitoring in real time, biofilm formation by bacteria on medical device surfaces, such that device colonisation can be intercepted before an infection develops. We chose polyvinyl chloride (PVC) ETTs as the demonstrator devices, due to their high infection rate susceptibility and outcome severity.[26] *P. aeruginosa* was chosen as the model pathogen, as attachment and subsequent biofilm formation by this pathogen is often implicated in device-centred infections.[9–11] LPG sensors were incorporated into the lumens of the ETTs for monitoring biofouling. LPG sensors can be considered as refractive index sensors; changes in medium refractive index near the sensor surface (including bacterial attachment and EPS production) cause measurable signal changes.[27,28] The ease of fabrication, low-level back reflection,[29] label free detection, low cost and the potential for multiplexing make LPG optical fibre sensors a potentially valuable option for monitoring biofilm formation in real time.

In this study, ETTs with an incorporated optical fibre sensor were investigated either uncoated or as a device coated with a biofilm resistant amphiphilic polymer[19] to investigate biofilm formation, with the intention of developing a sensitive method for the detection of early stage device colonisation. Through parallel monitoring of the wavelength shift of attenuation band(s) and 3D confocal microscopy of *P. aeruginosa* biofilm growth, the relationship between wavelength shift and biomass was established, validating the LPG optical fibre sensors as a method to quantify biofouling to facilitate the interception of device-centred infections.

Materials and methods

Materials

Ethylene glycol dicylcopentenyl ether acrylate (EGDPEA) and di (ethylene glycol) methyl ether methacrylate (DEGMA) monomers were supplied by Sigma Aldrich, UK. Solvents were obtained from Fisher Scientific, UK. Monomers and solvents were used as supplied. 2,2′-Azobis(2-methylpropionitrile) (AIBN, 98%) was obtained from Sigma Aldrich, UK and purified by recrystallization with methanol. Bis[(difluoroboryl) diphenylglyoximato] cobalt(II) (PhCobF) was obtained from DuPont and used as received. The silane primer (MED1-161) was supplied by NuSil Technology LLC, UK. Hi-Contour oral/ nasal cuffed endotracheal tubes were used, supplied by Mallinckrodt™ (Covidien). Tubes were adult size, with an inner diameter of 8 mm, outer diameter of 10.9 mm and maximum cuff diameter of 30 mm.

LPGs were fabricated in photosensitive boron-germanium co-doped optical fibres (Fibercore PS850), using custom made amplitude masks made of 1Cr18Ni9Ti steel alloy. LPGs were inscribed into a 3 cm length of the optical fibre using a frequency quadrupled Nd:YAG laser, emitting at 266 nm (Continuum minilite I). Optical fibres were acquired from Thorlabs Ltd (460HP, fibre ID: 10-C0157-20-4H-08). Optical fibres, with and without inscribed gratings, had core dimeters of 5 μm and fibre diameters of 125 μm, with the LPG grating period of 109 μm. The HL-2000 halogen light source, HR-4000 optical spectrometer, SubMiniature version A (SMA) connectors and the SpectraSuite software were obtained from Ocean Optics, UK.

Synthesis of EGDPEA:DEGMA polymer

240 mg AIBN, 100 mg PhCobF, 75.2 mL EGDPEA, 20.8 mL DEGMA and 200 mL toluene were combined and degassed with argon for 30 min, before heating at 80 °C for 24 h with stirring. Argon gas was flushed into the headspace of the reaction vessel throughout, to prevent early termination by oxygen. The polymer was then precipitated twice, by adding dropwise to cold hexane. Excess hexane was decanted and the remainder removed by vacuum drying the polymer at 0.11 Torr for 4 h. Aliquots of the final polymer product were analysed by gel permeation chromatography (GPC), using a PL-GPC 50 plus instrument (Agilent-Varian Inc., USA). The column used was a Polymer Labs PLgel guard column (50 × 7.5 mm, 8 μm), followed by a pair of PLgel Mixed-D columns (300 × 7.5 mm, 8 μm). Polystyrene (PS) was the standard used, with chloroform as the eluent. ^{1}H nuclear magnetic resonance (NMR) spectroscopy was also performed on EGDPEA and DEGMA monomers, the polymer crude mix and the purified polymer, in deuterated chloroform, using a Bruker AV400 spectrometer, operating at a frequency of 400.3 MHz. The ^{1}H NMR spectra allowed monomer conversion and feed ratio to be established.

Dip coating of LPG sensors and sensor-ETT systems

LPG optical fibres were fixed into the lumens of short ETT sections using autoclave tape. Sensor-ETT systems were left uncoated or dip coated in the MED1-161 silane primer and EDGPEA:DEGMA polymer solution, using a Holmarc HO-TH-01 dip coating unit (India). The system was first dipped into the silane adhesion promoter (primer), with the mechanical arm of the dip coating unit set to withdraw the system from the primer solution at 2 mm s^{-1}. The system was left to dry under ambient conditions for 30 min before it was dip coated in a 30% w/v solution of EGDPEA:DEGMA in dichloromethane (DCM). The polymer solution was made up by dissolving 15 g polymer in 50 mL DCM. The system was withdrawn from the polymer solution at 1 mm s^{-1}. After coating, the system was dried under ambient conditions for 24 h, then under vacuum (0.11 Torr) for a further 24 h.

Apparatus setup for spectra collection

Fig. S1† illustrates the setup of the sensor-ETT apparatus for spectra collection for the *P. aeruginosa* biofilm study. For the calibration in sodium chloride, the 3 cm sensitive region of the optical fibre sensor was placed in a specially designed PTFE well (7 × 1.9 × 1 cm, with a 4 cm long channel) without the ETT section. Only this sensitive region (fixed into the ETT section or into the PTFE well), uncoated or coated, was exposed to the relevant medium for spectra collection. Changes in refractive index at the sensor surface resulted in a change in the output transmission spectra, which was recorded by the spectrometer and displayed on the PC.

Sodium chloride calibration

The LPG optical fibre sensor was set up as illustrated in Fig. S1,† except the 3 cm sensitive region was placed in the

PTFE well. Sodium chloride solutions, ranging from 0 to 25% w/v (in 5% w/v increments) were made up by serial dilution from a 25% w/v stock in water. Each solution was then pipetted into the PTFE well separately, which held approximately 1.5 mL of liquid, and the transmission spectra recorded in the SpectraSuite software. This was done with both uncoated and coated LPG sensors.

P. aeruginosa strain and culture media

Biofilm experiments were carried out using the mCherry tagged fluorescent *P. aeruginosa* strain PA01-N (University of Nottingham collection) transformed with pME6032laclQΔ::mCherry[50] (containing a Tc^{r} selection marker). The *Pseudomonas aeruginosa* strain was streaked onto an LB (Luria–Bertani) agar plate supplemented with 125 μg mL^{-1} tetracycline and grown at 37 °C for 24 h, after which a single colony was taken and added to a centrifuge tube (Falcon) containing 5 mL growth medium using a sterile plastic loop. This centrifuge tube was incubated at 37 °C overnight, with shaking (200 rpm). The optical density at 600 nm (OD$_{600}$) was measured for the overnight culture and diluted in growth medium to achieve a final OD$_{600}$ of 0.05, with which the biofilm challenge experiments were carried out. For biofilm formation and sensor-ETT system measurements the following growth media were used; RPMI-1640 medium (R0883), obtained from Sigma Aldrich, UK and Artificial sputum medium[51] (ASM), prepared by following the method detailed by Palmer *et al.* (2007); see ESI,† 'Artificial Sputum Medium Composition'.

Sensor-ETT systems in bacterial culture media

The sensor-ETT apparatus (uncoated and silane primed and polymer coated) was set up as in Fig. S1,† with the section of ETT (plus the sensitive region of the sensor) placed into a Petri dish. The *P. aeruginosa* culture was prepared in ASM and the final culture medium added to the Petri dish, ensuring the instrumented ETT section was immersed in culture medium. A transmission spectrum was recorded at 0 h and the system left in place for 72 h. Transmission spectra were collected at 6 h intervals for 24 h, with additional readings taken at 48 and 72 h. The experiment was conducted at room temperature due to experimental restrictions.

Processing of transmission spectra and wavelength shift calculations

Spectra were collected in SpectraSuite and processed in OriginPro 8.6. A baseline was drawn over the raw spectra, omitting the attenuation peaks. The spectra were then divided by the baseline, resulting in a change in the axes from intensity *versus* wavelength to transmission percentage *versus* wavelength. This processing allowed for quantification of attenuation depth (loss of transmission) and attenuation peak wavelength. OriginPro 8.6 was then used to find the peak wavelengths, using the 'peak finder' function. The peak wavelength was the wavelength at which the highest loss of transmission occurred, *i.e.* the apex of the peak. Spectra processing and peak wavelength finding were performed on all collected

spectra, for both the calibration and the *P. aeruginosa* culture experiments, for both attenuation bands/peaks in the optical spectra. Wavelength shift was calculated for each peak using eqn (1):

$$\Delta\lambda = \lambda_{t/c} - \lambda_0 \tag{1}$$

where $\Delta\lambda$ is the wavelength shift, $\lambda_{t/c}$ is the peak wavelength at time t (for exposure to bacteria culture medium) or concentration c (for the sodium chloride calibration) and λ_0 is the peak wavelength at 0 h (bacteria) or 0% w/v (sodium chloride). Wavelength shift was then plotted against concentration or time respectively.

Confocal laser scanning microscopy (CLSM) of biofilms

1 cm^2 sections of ETT and 7.5 cm lengths of insensitive optical fibre were cut and cleaned by immersion in acetone. Half of samples were left uncoated and half were dip coated in the silane primer and a 30% w/v EGDPEA:DEGMA polymer solution in DCM (withdrawal speeds 2 mm s^{-1} and 1 mm s^{-1} respectively). After coating, samples were dried under ambient conditions for 24 h, then under vacuum (0.11 Torr) for a further 24 h. Samples were immersed in RPMI-1640 or ASM and inoculated with *P. aeruginosa*, in single well chamber slides (Nunc® Lab-Tek® II, Sigma Aldrich UK, for 72 h, at 37 °C or room temperature, allowing comparisons of temperature and media. At 6 h intervals (for 24 h, with further images obtained at 48 and 72 h), biofilms were imaged using a Zeiss LSM 710 confocal microscope (Carl Zeiss, Germany). Samples were left in the chamber slides during imaging. Chamber slides were placed under a 10× objective (NA = 0.3) and the wavelength of the Ar/Kr laser set at 555 nm, to excite fluorescent mCherry (excitation = 587 nm, emission = 610 nm).[52] The power of the laser was set at 15.0 arbitrary units (1.5 mW) and the gain of the 'mCherry' channel was kept between 800 and 900. *Z* stack images were taken for each sample; the upper and lower stacks were set by cycling through the axial range, in both directions, until no fluorescence was observed (or the image was out of focus). The stack at which no fluorescence was observed was set as the upper/lower stack. An average of 40 *Z* slices were taken for each image, with an average step height of 6.10 μm. The detector pinhole was optimised to 1 AU, which gave a pinhole size of 34.1 μm. Images were acquired and processed in the ZEN 2009 software. 2D and 3D images were taken, for display and biomass quantification respectively.

Quantification of biomass using COMSTAT

The ImageJ plugin, COMSTAT 2.1, was used for biomass quantification from the CLSM images.[33] All *Z* stack images were imported into COMSTAT from the ZEN software. A fluorescence threshold was required for biomass calculation. For the first image in the queue, the threshold was set to its minimum and gradually increased until only fluorescence associated with biomass was observed. This method ensured that any background fluorescence or low brightness pixels

associated with noise were removed. The threshold value was kept the same for the remaining images in the queue, ensuring any background contributions were the same for all images. The threshold was input into the COMSTAT menu and biomass selected for quantification. The software records the biomass as μm^3 μm^{-2}, which was then converted to μg cm^{-2} by multiplying by 100, assuming a biofilm density of 1 g cm^{-3} (biofilms are mainly composed of water).

Estimation of sensor sensitivity

The uncoated LPG optical fibre sensor was set up as illustrated in Fig. S1,† with the 3 cm sensitive region placed into the PTFE well (as with the sodium chloride calibration). *P. aeruginosa* cultures was prepared as previously in RPMI-1640 medium or ASM. 1.5 mL of culture medium were added to the PTFE well and a 0 h transmission spectrum recorded. The well was placed in a Petri dish of water, to prevent medium evaporation. The system was left for biofilms to form at room temperature. Transmission spectra were continuously monitored until a measurable wavelength shift of the attenuation bands occurred. Simultaneously, uncoated 1 cm^2 sections of ETT were exposed to the same *P. aeruginosa* cultures in RPMI-1640 or ASM at room temperature, in single well chamber slides (Nunc® Lab-Tek® II, Sigma Aldrich, UK). At the time when a measurable wavelength shift occurred, the chamber slides were placed under the Zeiss LSM 710 confocal microscope (Carl Zeiss, Germany). 2D and *Z* stack images were acquired of biofilms, using the same microscope configuration described above. The biomass was quantified in COMSTAT, after thresholding. These data allowed the sensitivity to biomass to be expressed as the smallest peak wavelength shift per unit biomass.

Results and discussion

Assessment of anti-biofilm polymer coating

Sections of ETT were left uncoated, or coated with a biofilm resistant polymer, poly(ethylene glycol dicyclopentenyl ether acrylate-*co*-diethylene glycol methyl ether methacrylate), which we will refer to as EGDPEA:DEGMA.[19] Adhesion between the coating and the ETT was facilitated using a silane adhesion promoter (primer). This was required since in the absence of the primer, the coating was not continuous or smooth over the entire ETT surface, and delaminated on incubation in growth media. After coating, the samples appeared smooth and continuous and we observed no signs of delamination, suggesting that the silane primer achieved stable adhesion[32] between the coating and the PVC of the ETT for the conditions used in this study. Furthermore, the coating remained completely smooth and continuous after at least 9 months of ambient storage, further demonstrating the stability of the adhesion between the polymer and ETT substrate.

Adhesion promoting silane primers contain chemical groups intended to bond with both substrate and coating functionalities, allowing improved adhesion between the materials.

In solution, the alkoxysilanes groups are hydrolysed to form reactive silanols.[57] The formulation contained a condensation catalyst, which causes the silanols to condense together.[58] These condensed silanols then form stable bonds with the substrate surface, *via* covalent bonds, for example. In the case of PVC, the silanols are unlikely to covalently bind to the pristine substrate due to a lack or reactive surface functionalities, but more likely form electrostatic interactions, such as hydrogen bonding with any oxidised surface moieties.[57,58]

The object labels/description of 'coated' represents samples that had been first silane primed and then polymer coated. The polymer was prepared using catalytic chain transfer radical polymerisation,[20] resulting in a polymer with a molecular weight of 1.8×10^4 g mol^{-1} and a polydispersity index of 1.6 (Table S1†). The polymer was applied to the ETT and optical fibre by dip coating, producing coatings with mean thicknesses of 0.6 and 0.5 µm respectively, excluding the primer layer (measured by weighing samples of known dimensions pre- and post-coating, and measuring the density of the polymer, which was 1.6 g cm^{-3}). Coated and uncoated samples were immersed in either RPMI-1640 or ASM inoculated with *P. aeruginosa* and incubated for 24 h at 37 °C or room temperature. Measurement at 37 °C was not physically possible for the full optical fibre instrumentation measurements in our category 2 containment setup. However, in clinical use, sensor electronics could readily be adapted for bedside application. RPMI-1640 is a standard laboratory medium that supports biofilm formation while ASM is an approximation to the ETT lumen in the tracheal environment. At 6 h intervals, the *P. aeruginosa* biofilm was imaged *in situ* using confocal laser scanning fluorescence microscopy and the biomass was quantified for both sample types as shown in Fig. 1 for the ETT lumen and Fig. 2 for the optical sensor fibre.

P. aeruginosa in RPMI-1640 is shown in Fig. 1 to display colonisation consistent with the initial bacterial attachment and early biofilm development over the first 6–12 h. Microcolonies were observed at 18 h, with biofilm architecture observed at 18 and 24 h, with a mean biomass at 24 h of 2923 µg cm^{-2}. Heydorn *et al.* commented that *P. aeruginosa* underwent a similar growth pattern, with cells colonising the substratum and forming flat, uniform biofilms, over 24 h.[33] This also occurs in ventilator associated pneumonia, with rapid colonisation of ETTs *in situ*, followed by dispersal and aerosolisation of microorganisms in the lower airways within 48 h of initiating intubation.[12,13] The polymer coating reduced biofilm formation (mean biomass at 24 h of 354 µg cm^{-2}) with large uncolonized areas of the ETT section clearly apparent. After 24 h, little biofilm was apparent compared with the uncoated PVC substrate. The polymer therefore clearly inhibits biofilm development under optimal experimental conditions for biofilm formation.

In ASM, *P. aeruginosa* biofilm formation on the uncoated ETT sections was either delayed or incomplete, as the images revealed many more isolated patches compared with those in RPMI-1640 (Fig. 1), with only a few microcolonies observed.[31] The 24 h biomass values were 2923 v 443 µg cm^{-2}, RPMI-1640

v ASM, on the uncoated substrates. The coated ETT showed no detectable biofilm formation, and zero biomass was recorded. This highlights the anti-biofilm properties of EGDPEA: DEGMA. It is likely that a low level of cellular attachment occurred on the coated sample in ASM, albeit below the limit of detection of the confocal system.

The same pattern was observed on the optical fibres in Fig. 2, with a greater biomass forming in RPMI-1640 compared to ASM on the equivalent surface-treated sample (uncoated or coated). The polymer coating also reduced biofilm formation in a similar manner, again with no biomass recorded on the coated sample in ASM. No biofilm was observed on the coated samples (zero biomass recorded).

Because of physical experimental constraints, the optical fibre sensing experiment was undertaken at room temperature. Equivalent ETT and optical fibre samples (uncoated and coated) were exposed to *P. aeruginosa* in ASM at room temperature, with images taken and biomass quantified at 6 h intervals for the first 24 h presented in Fig. S2.† This was to capture quantitative confocal data in the same environment of the ETT-sensor apparatus when collecting the spectral data from the optical sensor. Similar trends were observed to the 37 °C incubation but with much less well developed biofilms. Lesser biofilm development was observed at room temperature than at 37 °C for the equivalent sample. This is because *P. aeruginosa* biofilm formation is known to be strongly affected by temperature.[7–10]

The effectiveness of EGDPEA:DEGMA in resisting biofilm formation on different surfaces, including the PVC of ETTs and silica of optical fibres, is demonstrated in Fig. 1 and 2. It could therefore be used as an inexpensive coating for breathing tubes, to prevent the attachment and growth of potentially harmful bacteria such as *P. aeruginosa*, which may cause illnesses such as ventilator-associated pneumonia (VAP). Fig. 3 summarises the workings of the coating.

LPG sensor response in *P. aeruginosa* cultures

The principles of LPG optical fibre sensors are detailed in the ESI† 'LPG optical fibre sensor considerations'. In brief, attenuation bands arise when light couples from the core mode into co-propagating cladding modes.[34–36] Changes in refractive index near the sensor's cladding surface caused a change in the effective refractive index of the cladding modes,[27,28] resulting in coupling to occur at different wavelengths and a wavelength shift (x axis shift) of the attenuation bands/peaks (Fig. 4).[53]

To assess the ability to monitor bacterial biofilm formation in real time, LPG optical fibre sensors were incorporated into the lumen of sections of ETT, immersed in ASM inoculated with *P. aeruginosa* and left for 24 h at room temperature. Upon immersion in bacterial culture, two attenuation bands (peaks) were observed in the optical spectrum (Fig. 4). *P. aeruginosa* biofilms were then allowed to form on substrate surfaces for 24 h and optical spectra were collected at 6 h intervals. The wavelength shift ($\Delta\lambda$) was calculated for both attenuation peaks. The results for peak 2 are displayed in Fig. 4. Peak
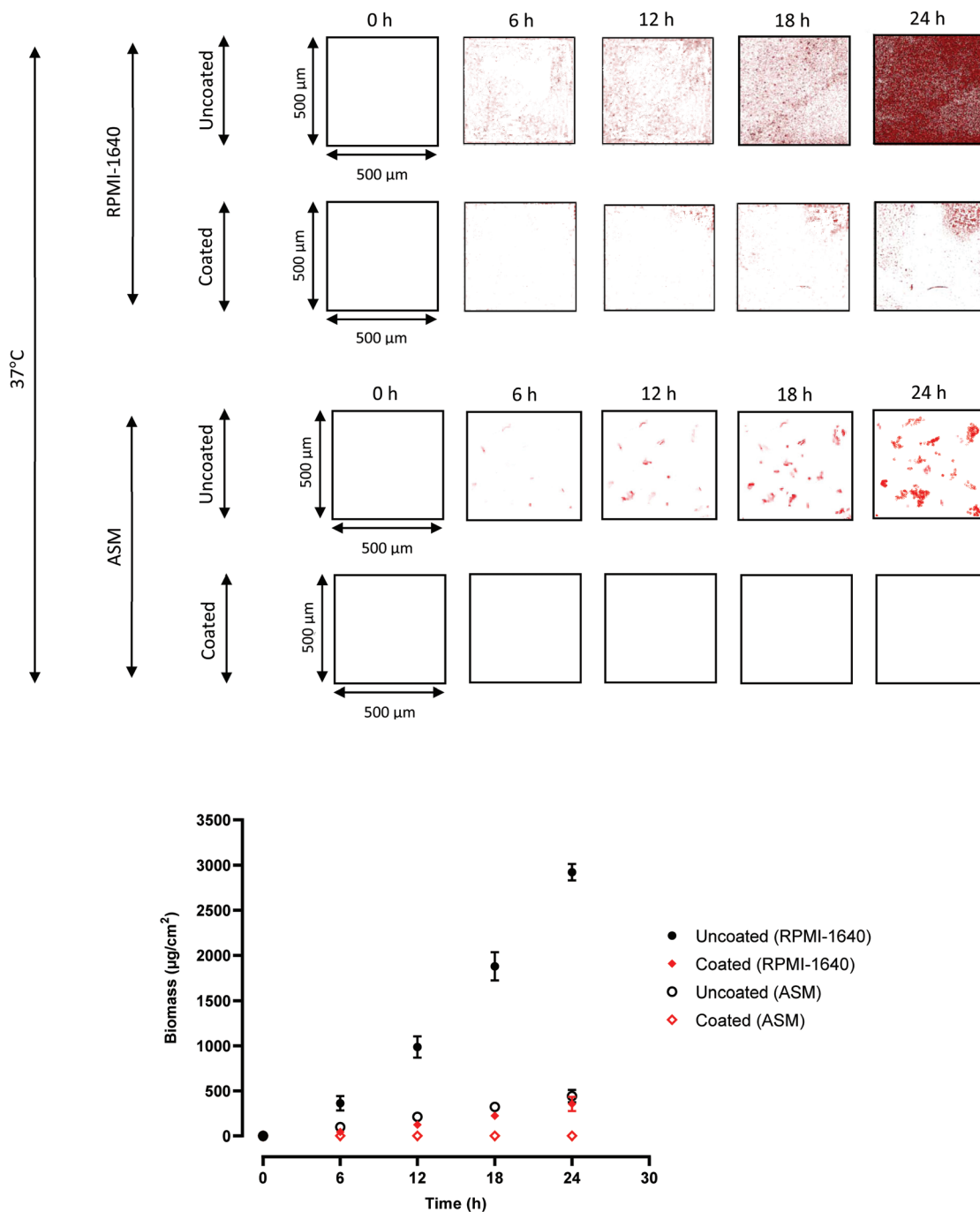
Fig. 1 Confocal microscopy quantification of *P. aeruginosa* biofilms in ETT sections. 2D confocal images of *P. aeruginosa* biofilms on uncoated and coated ETTs at 6 h intervals for 24 h, at 37 °C, in RPMI-1640 and ASM. The red areas represent biofilm, as the *P. aeruginosa* was transformed to express fluorescent mCherry (excitation = 587 nm, emission = 610 nm). All images are 500 × 500 μm. Quantification of biomass for all images, using COMSTAT, with a fluorescence threshold of 56 AU. Points are mean biomass $\pm$ s.d., $N = 3$.

2 gave a positive correlation between $\Delta\lambda$ and time, so the peak 2 wavelength shift was plotted against the inverse of biomass and an exponential trend fitted over the data points (Fig. 4). The equivalent peak 1 data is shown in Fig. S11.†

Both attenuation peaks shifted linearly with increased time of immersion in bacteria cultures ($R^2 = 0.98$ for both peaks, Fig. 4) and shifted in opposite directions. The coated sensor-

ETT system displayed zero wavelength shift at all time points, as the attenuation band did not change its x position during the entirety of the exposure time. This indicates that the polymer coating inhibited biofilm formation to the extent that the refractive index change was below the limit of detection of the sensor. After 24 h, the wavelength shift from the uncoated system was significantly higher than the coated system, for both peaks. The
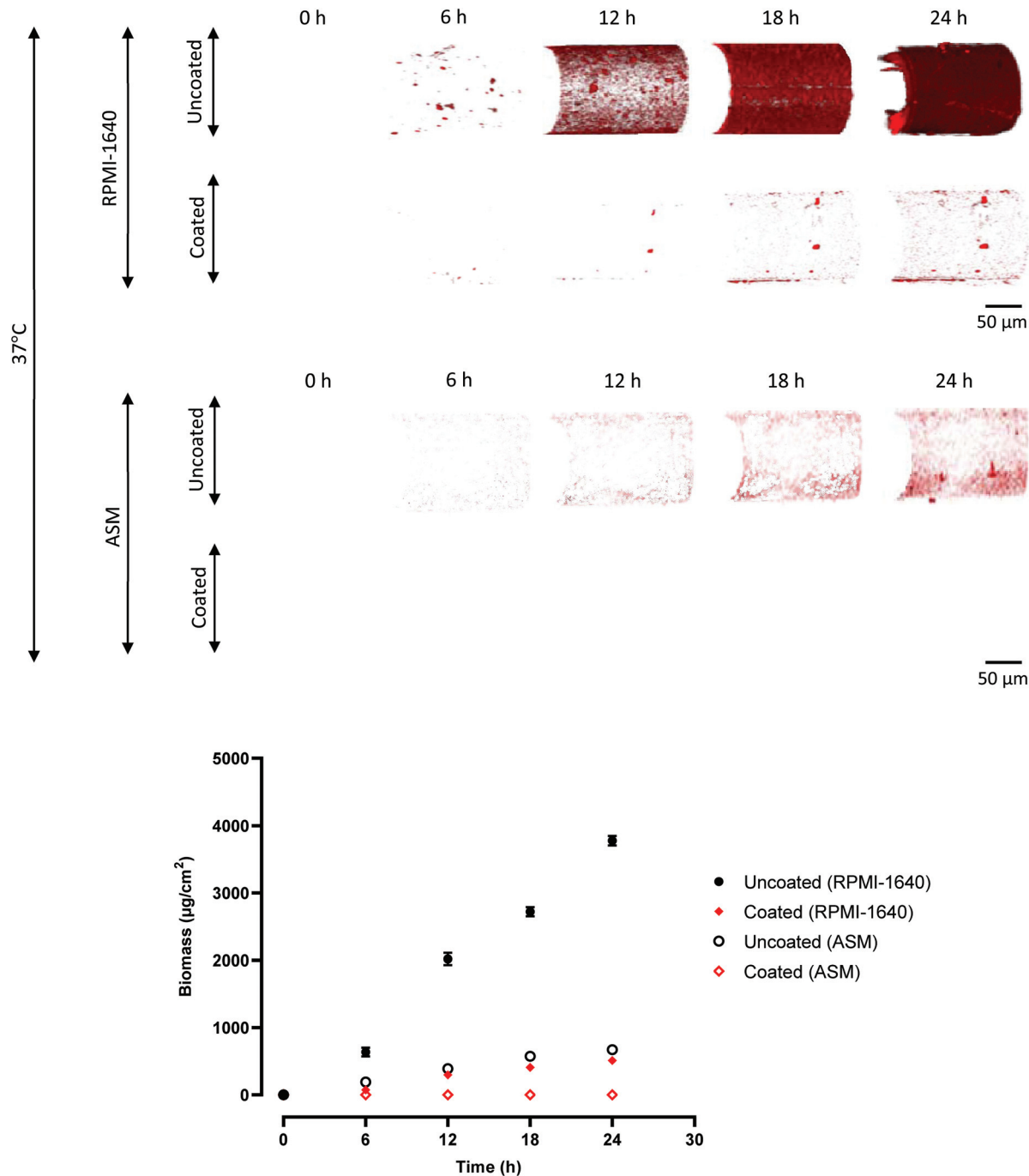
Fig. 2 Confocal microscopy quantification of *P. aeruginosa* biofilms on optical fibres. 3D confocal images of *P. aeruginosa* biofilms on uncoated and coated optical fibres at 6 h intervals for 24 h, at 37 °C, in RPMI-1640 and ASM. The red areas represent biofilm, as the *P. aeruginosa* was transformed to express fluorescent mCherry (excitation = 587 nm, emission = 610 nm). The scale bar is 50 μm for all images. Quantification of biomass for all images, using COMSTAT, with a fluorescence threshold of 56 AU. Points are mean biomass ± s.d., $N = 3$.

strong exponential correlation ($R^2 = 0.94$) observed between the inverse of biomass and the spectral response ($\Delta\lambda$) demonstrated that the wavelength shift could be used as an accurate measurement of bacterial biofilm formation (Fig. 4).

Critically, when the equivalent experiment was repeated in the more biofilm supportive RPMI-1640 growth medium (also at room temperature), the wavelength shift increase was greater on uncoated systems (Fig. S10†). This indicates a greater increase in refractive index *via* biofilm formation. This was corroborated by the increase in surface coverage and quantified biomass (Fig. 1, albeit at 37 °C). The LPG optical fibre sensor can detect biofilm growth, with higher wavelength shifts representing biofilms of higher biomass. Hence, the system can be used to quantify biomass at any given time
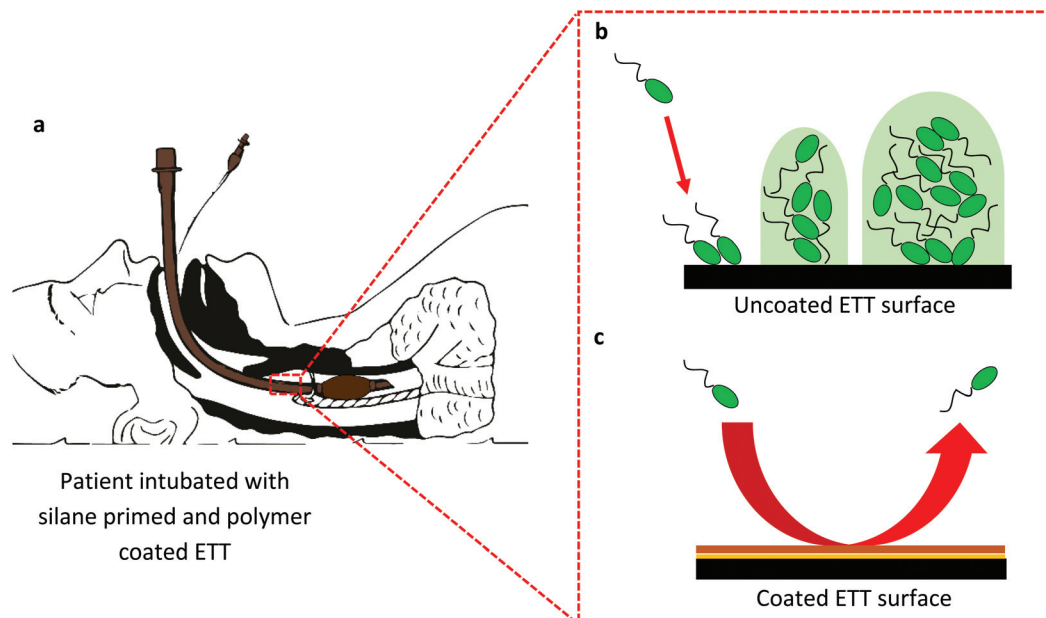
Fig. 3 Assessment of biofilm resistant polymer *in situ*. (a) A patient intubated with an EGDPEA:DEGMA coated ETT. (b) Bacterial attachment and biofilm formation on an uncoated ETT surface. (c) The polymer coating reduces bacterial attachment to an ETT surface.

point, providing the system (medium and temperature) is first trained and the refractive index change is above the limit of detection of the sensor. Biofilm formation in the room temperature experiments was not as extensive as at 37 °C and so a calibration of the sensor results to more effective colonisation is important to consider when viewing these results.

Prior to the exposure of the optical sensor to bacteria culture media, uncoated and coated sensors were calibrated by exposing them to solutions of increasing concentration of sodium chloride in water (Fig. S7†). There were no differences observed in wavelength shift between the two sensors, suggesting that the polymer coating did not significantly reduce the sensitivity of the optical sensor. Also, before the experiment, both sensors were left immersed in RPMI-1640 and ASM separately without *P. aeruginosa* cells for 24 h, at room temperature, to ensure the equilibration of the system (temperature and absorbents) prior to interactions with bacteria. No change in wavelength shift was observed for both sensors during the equilibration period.

The linear increase in wavelength shift for the attenuation peaks was likely due to a change in refractive index at the surface of the sensor[37,38] as a result of bacterial biofilm formation. On coated systems, no wavelength shift was observed, indicating low biofilm formation, which is consistent with previous studies.[19,20] Some cells may have attached, but at a level below the refractive index limit of detection of the LPG sensor (estimated to be 0.001 refractive index units).[54–56] The detection of bacteria by the sensor was limited to the region of the evanescent field,[39–42] which, for the sensors used in this study, was greater than 0.5 μm from the cladding surface (see ESI,† 'LPG optical fibre sensor considerations'). However, the ability of the sensor to detect biofilm formation beyond the evanescent

field (which encompasses most of the biomass detected) could be due to larger colonies introducing a third waveguide (other than the core and cladding), which created another coupling condition.[63] In brief, the additional waveguide acts as another layer of the optical fibre sensor, allowing light mode coupling at distances greater than the evanescent field.[40–42,63]

The optical density (OD at 600 nm) of the bulk growth medium was measured after bacterial inoculation at intervals over a 24 h period, comparing uncoated and coated samples. No significant differences were observed in the planktonic bacterial population density after 24 h between the uncoated and coated ETT systems, where biofilm formed only on the uncoated sample. Since the refractive index change and subsequent wavelength shift was only apparent in the presence of biofilm, we can conclude that the sensor is responding specifically to the biofilm and not to the planktonic cells. This is likely due to the planktonic cells having a negligible difference in refractive index to the medium.[64] The refractive index change in the bulk growth medium (containing planktonic cells) is therefore significantly less than that in the sodium chloride solutions used for the calibration, which caused a measurable wavelength shift (Fig. S7†).

Judicious positioning of the sensor is required to ensure that the chances of detecting biofilm-mediated infection are maximised (Fig. 4). It has been observed that the heaviest colonisation occurs on the luminal surface of the ET tube,[43] this is also the area when air flow occurs providing opportunity for bacterial dispersal into the lungs, hence positioning of the sensor in the lumen would maximise its sensitivity to detect and allow interception of bacterial colonisation of ETTs. This also removes potential complications arising from contact of the sensor with the tracheal wall.
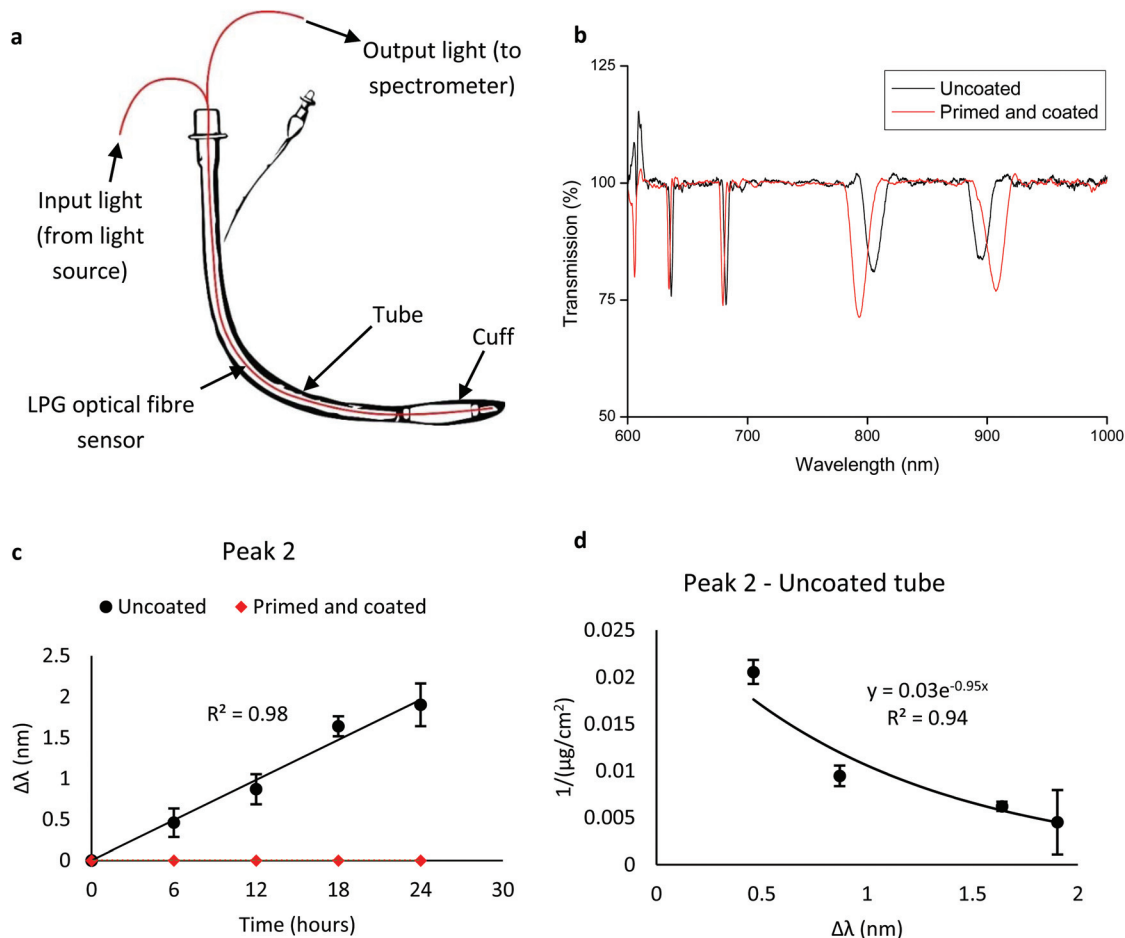
Fig. 4 Response from LPG sensor instrumented ETT. (a) Schematic of prototype ETT, with LPG sensor incorporated into the lumen. (b) Processed optical (transmission) spectrum from uncoated and coated LPG sensors immersed in *P. aeruginosa* cultures at 0 h, at room temperature. Two attenuation bands/peaks are present, labelled 'Peak 1' and 'Peak 2'. (c) Wavelength shift ($\Delta\lambda$) of peak 2 from uncoated and coated LPG sensor-ETT systems immersed in *P. aeruginosa* in ASM for 24 h, at room temperature. Error bars are $\pm$s.d., N = 3. (d) Plot of peak 2 wavelength shift from (c) against the inverse biomass of *P. aeruginosa* biofilms grown on uncoated ETT sections in ASM, at room temperature (Fig. S2†). An exponential function is fitted to the data. Error bars are $\pm$s.d., determined from 3 biological replicates.

The confocal fluorescence images (Fig. 1 and 2) showed architectural differences between the biofilms grown in the two media, and between the uncoated and coated samples. On the uncoated sample in RPMI-1640 (at 37 °C), *P. aeruginosa* formed uniform, flat biofilms, whereas on the coated sample and in ASM (at 37 °C and room temperature), patchy areas of biomass were observed. This is not unusual, as biofilm growth often begins by densely colonising areas of the substratum.[33] This provides some insights into the differences between the growth media, whereby the nutrient composition provided differing environments for biofilm formation.

Although this response is observed in the *in vitro* environment, it is also possible to train the sensor system to operate *in vivo*. There will be differences in the growth profile of biofilms *in vivo*, since the ETT lumen is subjected to warm, moist, oxygenated air when in use.[22] However, the LPG sensor only detects changes in refractive index (of the biofilm), hence, if the system could be calibrated in that environment, a sensor-instrumented ETT could be used to monitor biofilm growth *in vivo*.

Wavelength shift-biomass relationship and sensitivity of LPG sensor to biomass

Establishing a correlation between the wavelength shift and biomass was key to enabling the optical sensor to report quantitative measurements of biofilm development. Here we note that the biomass measured in this study was associated with the bacteria, and the refractive index change was caused by the developing biofilm. We observed a strong exponential correlation between the wavelength shift and the inverse of biomass, (R^2 = 0.94 and 1.00, peak 2 and 1 respectively, Fig. 4 and S11†), which can be used to estimate the biomass from the wavelength shift alone (of peak 2), by using the equation:

$$y = 1/(0.03e^{-0.95x})$$

where y is the biomass (μg cm^{-2}) and x is the wavelength shift. This exponential function was only applicable to the uncoated sensor-ETT system, as there was no recorded biomass or wavelength shift on the coated system after culturing with bacteria.

However, the similar response of the coated and uncoated sensors to NaCl solutions of increasing concentration (and refractive index) suggests that the above equation could also be applied to the coated sensor.

A measurable wavelength shift from the uncoated sensor-ETT system, in RPMI-1640 inoculated with *P. aeruginosa*, at room temperature, occurred after 1 h; the wavelength shifts of peaks 1 and 2 at this time were −0.52 nm and 0.17 nm respectively. The biomass of the *P. aeruginosa* biofilm formed on uncoated ETT sections in the same culture environment after 1 h was 81 µg cm^{-2}. The sensitivity of the LPG OFS to biomass can be expressed as the smallest wavelength shift per biomass unit,[30] which is 0.002 nm µg^{-1} cm^{-2}. The limit of detection is therefore 81 µg cm^{-2}.

In ASM, a wavelength shift was measured after 5 h. The peak 1 and 2 wavelength shifts at 5 h were −0.55 and 0.30 nm respectively. The biomass on uncoated optical fibres after 5 h was 71 µg cm^{-2} (Fig. S12†). The smallest wavelength shift per biomass unit was 0.004 nm µm^{-3} µm^{-2}, with a limit of biomass detection of 71 µg cm^{-2}. The LPG sensor therefore had a lower biomass detection limit in ASM, but a lower wavelength resolution. Media which promote biofilm formation tend to give higher wavelength resolution and earlier detection times, but due to the rapid formation of biofilm, a higher biomass detection limit. It also appears that the limit of detection of the confocal microscope system for these conditions was 71 µg cm^{-2}.

Due to the high sensitivity to biomass and the low limit of detection, LPG sensors could be a suitable instrumentation for ETTs to provide live, accurate feedback on device colonisation. The limit of detection in respect to refractive index depends on the grating period and core diameter of the LPG,[28,29] but can be quantified by measuring the refractive index of the biofilm itself,[44,45] a future consideration.

Design of a sensor-instrumented ETT

Within this study, the measurements were taken from the LPG sensor by passing light through the sensor; the analysis beam was directed through one end of the optical fibre and detected at the other end. For application in an ETT both the analysis
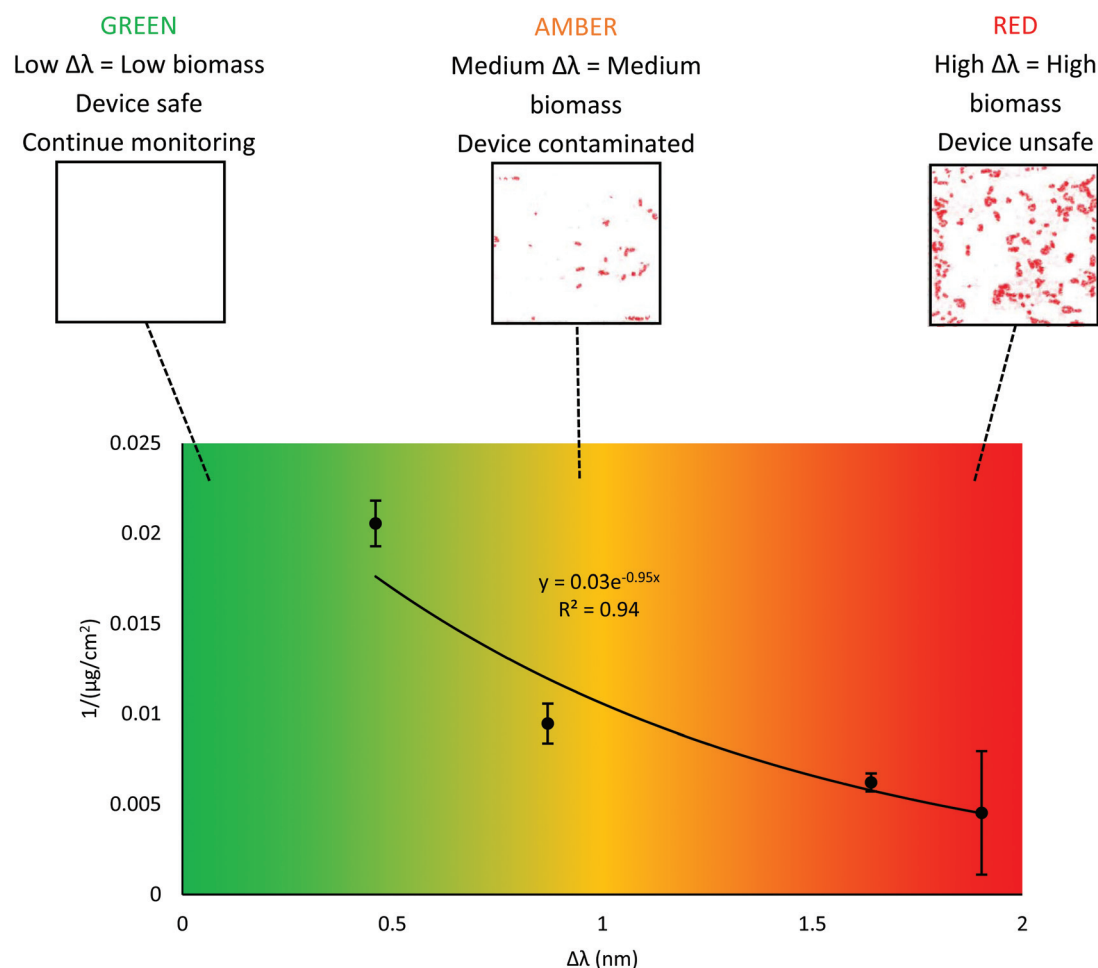

Fig. 5 Traffic light system for infection prediction. Relationship between peak 2 wavelength shift (Δλ) and inverse biomass for the uncoated LPG sensor-ETT system, exposed to *P. aeruginosa* in ASM for 24 h, at room temperature. Error bars are ±s.d. of biomass, *N* = 3. A traffic light colour scheme indicates the 'safety' of the device, predicted by the Δλ only. In the confocal images, the red areas represent biofilm, since the *P. aeruginosa* strain was transformed to express fluorescent mCherry (excitation = 587 nm, emission = 610 nm). Images are 500 µm × 500 µm.

and detection would need to be at the same end of the optical fibre. This can be easily achieved using a reflective tip on the optical fibre, to reflect the input light back up the fibre to the spectrometer.[46] The optical fibre sensor could be incorporated into the lumen of an ETT, using safe and approved adhesives, such as the cyanoacrylates,[47] or incorporate into the body of the tube in the same manufacturing step as the tube. We would envisage coating the device with EGDPEA:DEGMA, to minimise the risk of bacterial attachment and subsequent biofilm formation. The LPG sensor is also sensitive to temperature and strain on the fibre, which could be compensated using a reference LPG.[34–37]

In the clinic, the instrumented ETT (Fig. 4) would provide a constant readout of wavelength shift, which can then be used to estimate the biomass of any biofilm on the surface of the device. Through clinical testing, the readout could be calibrated to relate to clinical outcomes, which can be classified using a 'traffic light' system. Green would indicate that the biomass is sufficiently low so as to suggest no infection and the device can continue to be used, amber would indicate that there is evidence to suggest a biofilm is developing and that the patient should be closely monitored, whilst red would indicate that an infection has developed and that the device should be removed (Fig. 5). Presently, this system is arbitrary and requires the quantified biomass on ETT surfaces to be correlated to clinical outcomes, *via* human trials, such that the traffic light colours provide clinical information to physicians. Fig. 5 illustrates how such a system could be used *in situ*.

The advantages of this system are that the infection risk can be assessed in real time and *in situ*, without the need of device removal and time-consuming analysis. This reduces the incidence of unnecessary ETT replacement, whilst ensuring ETTs are replaced before a device infection can further develop into VAP. Furthermore, LPG optical fibre sensors can be fabricated inexpensively, and the associated hard/software are low cost. This makes the instrumented ETT an attractive proposition for healthcare services and intensive care units. Thus, we see opportunities for a similar coating and instrumented interception strategies for other indwelling medical devices.

Non-specificity of optical sensor and detection of biofilm loss

Since the LPG optical fibre sensor is a refractive index sensor, it cannot distinguish between different bacterial species, hence it is not a species specific sensor.[34–36] We used *P. aeruginosa* as an exemplar in this study, due to its involvement in ETT associated infections and VAP,[8,9] to demonstrate the sensitivity and efficacy of the optical sensor. This non-specificity enhances its potential utility as a biofilm-sensing instrument for medical devices, where ensuing infection is often caused by multiple species.[48] The traffic light system illustrated in Fig. 5 is therefore a generalised approach to biofilm detection and clinical intervention, which could be made specific to multiple and mixed bacteria through clinical evaluations, allowing tailored treatments to be administered accordingly.

The sensor was also able to detect, in real time, the loss of biofilm from the device surface, which occurred between 24 and 48 h after bacterial exposure. The depletion of nutrients over time in the growth medium caused biofilm disintegration/dispersion and cell death,[49] resulting in a reversal of wavelength shift, or a return of wavelength shift to zero. This was corroborated by a fall in biomass to zero, measured from confocal images (Fig. S14†) at 24 and 48 h. This could be useful as an *in situ* method of monitoring the effectiveness of patient/device treatment strategies, such as antibiotic treatment.

Conclusion

Device-associated infections, including VAP, remain an unmet healthcare problem that requires multi-facetted solutions. In this study, a novel anti-biofilm polymer has been successfully applied to an ETT to greatly reduce *P. aeruginosa* biofilm formation for at least 24 h of immersion in an optimal biofilm formation culture medium, and a sputum model of the ETT lumen. Furthermore, we incorporated an optical fibre sensor to enable the real time measurement of biofilm development at the surface of an ETT. A reproducible exponential relationship between the optical signal and biomass was observed, allowing the optical sensor to quantitatively report the amount of biomass. Together, a sensor instrumented ETT coated with an anti-biofilm polymer is a powerful tool suitable for clinical application that reduces biofilm development and associated device-related infections whilst providing physicians with live, *in situ* feedback on bacterial colonisation of the device, enabling for informed clinical strategies to be implemented. The application of this device has the potential to reduce patient morbidity and mortality and to lower infection treatment costs to healthcare services. The sensor technology and anti-biofilm polymer can be extended to other medical devices, where bacterial colonisation pose significant healthcare issues.

Data availability

The data supporting the findings of this study are available within the paper and ESI.†

Author contributions

Y.K. performed the experiments that gave the resulting data presented in this report. Y.K., S.K. and S.P.M. designed the studies involving the LPG sensors, including the calibration, sensor-ETT system design and the sensitivity test. Y.K. and S.K. designed the prototype ETT device for future testing. Y.K., J.F.D., P.W. and A.L.H. designed the biofilm assays and prepared the *P. aeruginosa* cultures. Y.K., A.L.H., D.H. and M.R.A. designed the protocol for polymer synthesis, dip coating samples and testing the system *in vitro*. All authors contributed to manuscript writing.

Conflicts of interest

The authors declare no competing financial interests.

Acknowledgements

References

1 J. Chastre and J. Y. Fagon, Ventilator-associated pneumonia, *Am. J. Respir. Crit. Care Med.*, 2002, **165**, 867–903.

2 J. W. Costerton, Z. Lewandowski, D. E. Caldwell, D. R. Korber and H. M. Lappin-Scott, Microbial biofilms, *Annu. Rev. Microbiol.*, 1995, **49**, 711–745.

3 R. M. Donlan, Biofilms: Microbial Life on Surfaces, *Emerging Infect. Dis.*, 2002, **8**, 881–890.

4 J. W. Costerton, G. G. Geesey and K. J. Cheng, How bacteria stick, *Sci. Am.*, 1978, **238**, 86–95.

5 T. F. Mah, B. Pitts, B. Pellock, G. C. Walker, P. S. Stewart and G. A. O'Toole, A genetic basis for Pseudomonas aeruginosa biofilm antibiotic resistance, *Nature*, 2003, **426**, 306–310.

6 K. Sauer, A. K. Camper, G. D. Ehrlich, J. W. Costerton and D. G. Davies, *Pseudomonas aeruginosa* displays multiple phenotypes during development as a biofilm, *J. Bacteriol.*, 2002, **184**, 1140–1154.

7 J. L. Vincent, D. J. Bihari, P. M. Suter, H. A. Bruining, J. White, *et al.*, The prevalence of nosocomial infection in intensive care units in Europe, *J. Am. Med. Assoc.*, 1995, **274**, 639–644.

8 T. Rasamiravaka, Q. Labtani, P. Duez and M. El Jaziri, The Formation of Biofilms by *Pseudomonas aeruginosa*: A Review of the Natural and Synthetic Compounds Interfering with Control Mechanisms, *BioMed Res. Int.*, 2015, **2015**, 1–17.

9 C. E. Davies, K. E. Hill, M. J. Wilson, P. Stephens, C. M. Hill, *et al.*, Use of 16S ribosomal DNA PCR and denaturing gradient gel electrophoresis for analysis of the microfloras of healing and nonhealing chronic venous leg ulcers, *J. Clin. Microbiol.*, 2004, **42**, 3549–3557.

10 R. J. Koerner, Contribution of endotracheal tubes in the pathogenesis of ventilator-associated pneumonia, *J. Hosp. Infect.*, 1997, **2**, 83–89.

11 S. Esposito, S. M. Purrello, E. Bonnet, A. Novelli, F. Tripodi, *et al.*, Central venous catheter-related biofilm infections: An up-to-date focus on meticillin-resistant *Staphylococcus aureus*, *J. Glob. Antimicrob. Resist.*, 2013, **1**, 71–78.

12 M.H Kollef, C.W Hamilton and F.R Ernst, Economic impact of ventilator-associated pneumonia in a large cohort study, *Infect. Control Hosp. Epidemiol.*, 2012, **33**, 250–256.

13 A. Amin, Clinical and Economic Consequences of Ventilator-Associated Pneumonia, *Clin. Infect. Dis.*, 2009, **49**, 36–43.

14 H. Saini, S. Chhibber and K. Harjai, Antimicrobial and anti-fouling efficacy of urinary catheters impregnated with a combination of macrolide and fluoroquinolone antibiotics against *Pseudomonas aeruginosa*, *Biofouling*, 2016, **32**, 511–522.

15 N. K. Shapur, M. Duvdevani, M. Friedman, B. Zaks, I. Gati, *et al.*, Sustained release varnish containing chlorhexidine for prevention of biofilm formation on urinary catheter surface: in vitro study, *J. Endourol.*, 2012, **26**, 26–31.

16 M. H. Kollef, B. Afessa, A. Anzueto, C. Veremakis, K. M. Kerr, *et al.*, Silver-coated endotracheal tubes and incidence of ventilator-associated pneumonia: the NASCENT randomized trial, *J. Am. Med. Assoc.*, 2008, **300**, 805–813.

17 P. Kingshott, J. Wei, D. Bagge-Ravn, N. Gadegaard and L. Gram, Covalent Attachment pf Poly(ethylene glycol) to Surfaces, Critical for Reducing Bacterial Adhesion, *Langmuir*, 2003, **19**, 6912–6921.

18 L. Zhang, Z. Cao, T. Bai, L. Carr, J. R. Ella-Menye, *et al.*, Zwitterionic hydrogels implanted in mice resist the foreign body reaction, *Nat. Biotechnol.*, 2013, **31**, 553–556.

19 A. L. Hook, C. Y. Chang, J. Yang, J. Luckett, A. Cockayne, *et al.*, Combinatorial discovery of polymers resistant to bacterial attachment, *Nat. Biotechnol.*, 2012, **30**, 868–875.

20 K. Adlington, N. T. Nguyen, E. Eaves, J. Yang, C. Y. Chang, *et al.*, Application of Targeted Molecular and Material Property Optimization to Bacterial Attachment-Resistant (Meth)acrylate Polymers, *Biomacromolecules*, 2016, **17**, 2830–2838.

21 R. A. Weinstein, M. J. M. Bonten, M. H. Kollef and J. B. Hall, Risk Factors for Ventilator-Associated Pneumonia: From Epidemiology to Patient Management, *Clin. Infect. Dis.*, 2004, **38**, 1141–1149.

22 I. A. Pneumatikos, C. K. Dragoumanis and D. E. Bouros, Ventilator-associated Pneumonia or Endotracheal Tube-associated Pneumonia? An Approach to the Pathogenesis and Preventive Strategies Emphasizing the Importance of Endotracheal Tube, *Anesthesiology*, 2009, **110**, 673–690.

23 D. Honeybourne, J. C. Costello and C. Barham, Tracheal damage after endotracheal intubation: comparison of two types of endotracheal tubes, *Thorax*, 1982, **37**, 500–502.

24 P.N Abadian, N. Tandogan, J.J Jamieson and E.D Goluch, Using surface plasmon resonance imaging to study bacterial biofilms, *Biomicrofluidics*, 2014, **8**, 021804.

25 A. Pranzetti, S. Salaun, S. Mieszkin, M. E. Callow, J. A. Callow, *et al.*, Model Organic Surfaces to Probe Marine Bacterial Adhesion Kinetics by Surface Plasmon Resonance, *Adv. Funct. Mater.*, 2012, **22**, 3672–3681.

26 F. D. Sottile, T. J. Marrie, D. S. Prough, C. D. Hobgood, D. J. Gower, *et al.*, Nosocomial pulmonary infection: possible etiologic significance of bacterial adhesion to endotracheal tubes, *Crit. Care Med.*, 1986, **14**, 265–270.

27 L. Marques, F. U. Hernandez, S. W. James, S. P. Morgan, M. Clark, *et al.*, Highly sensitive optical fibre long period grating biosensor anchored with silica core gold shell nanoparticles, *Biosens. Bioelectron.*, 2016, **75**, 222–231.

28 T. Erdogan, Cladding-mode resonances in short- and long-period fiber grating filters, *J. Opt. Soc. Am. A*, 1997, **14**, 1760–1773.

29 H. Chen and Z. Gu, Filtering characteristics of film-coated long-period fiber gratings operating at the phase-matching turning point, *Optik*, 2014, **125**, 6003–6009.

30 F. Chiavaioli, C. A. J. Gouveia, P. A. S. Jorge and F. Baldini, Towards a Uniform Metrological Assessment of Grating-Based Optical Fiber Sensors: From Refractometers to Biosensors, *Biosensors*, 2017, **7**, 23.

31 M. Hu, T. C. Zhang, J. Stansbury, J. Neal and E. J. Garboczi, Determination of Porosity and Thickness of Biofilm Attached on Irregular-Shaped Media, *J. Environ. Eng.*, 2013, **139**, 923–931.

32 W. D. Bascom, Structure of Silane Adhesion Promoter Films on Glass and Metal Surfaces, *Macromolecules*, 1972, **5**, 792–798.

33 A. Heydorn, A. T. Nielsen, M. Hentzer, C. Sternberg, M. Givskov, *et al.*, Quantification of biofilm structures by the novel computer program COMSTAT, *Microbiology*, 2000, **146**, 2395–2407.

34 C. A. J. Gouveia, J. M. Baptista and P. A. S. Jorge, *Refractometric Optical Fiber Platforms for Label Free Sensing, Current Developments in Optical Fibre Technology*, InTech, Madeira, 2013.

35 V. Bhatia and A. M. Vengsarkar, Optical fiber long-period grating sensors, *Opt. Lett.*, 1996, **21**, 692–694.

36 S. W. James and R. P. Tatam, Optical fibre long-period grating sensors: characteristics and applications, *Meas. Sci. Technol.*, 2003, **14**, 49–61.

37 S. W. James, S. M. Topliss and R. P. Tatam, Properties of Length-Apodized Phase-Shifted LPGs Operating at the Phase Matching Turning Point, *J. Lightwave Technol.*, 2012, **30**, 2203–2209.

38 S. C. Cheung, S. M. Topliss, S. W. James and R. P. Tatam, Response of fibre optic long period gratings operating near the phase matching turning point to the deposition of nanostructured coatings, *J. Opt. Soc. Am. B*, 2008, **25**, 897–902.

39 P. H. Paul and G. Kychakoff, Fiber-optic evanescent field absorption sensor, *Appl. Phys. Lett.*, 1987, **51**, 12–14.

40 P. S. Kumar, C. P. G. Vallabhan, V. P. N. Nampoori, V. N. Sivasankara Pillai and P. Radhakrishnan, A fibre optic evanescent wave sensor used for the detection of trace nitrites in water, *J. Opt. A: Pure Appl. Opt.*, 2002, **4**, 247–250.

41 M. Ohtsu and H. Hori, *Near-Field Nano-Optics. From basic principles to nano-fabrication and nano-photonics*, Springer, New York, 1999.

42 A. Messica, A. Greenstein and A. Katzir, Theory of fiberoptic, evanescent-wave spectroscopy and sensors, *Appl. Opt.*, 1996, **35**, 2274–2284.

43 S. M. Koenig and J. D. Truwit, Ventilator-Associated Pneumonia: Diagnosis, Treatment, and Prevention, *Clin. Microbiol. Rev.*, 2006, **19**, 637–657.

44 M. Smietana, W. J. Bock, P. Mikulic, A. Ng, R. Chinnappan, *et al.*, Detection of bacteria using bacteriophages as recognition elements immobilized on long-period fiber gratings, *Opt. Express*, 2011, **19**, 7971–7978.

45 S. M. Tripathi, W. J. Bock, P. Mikulic, R. Chinnippan, A. Ng, *et al.*, Long period grating based biosensor for the detection of *Escherichia coli* bacteria, *Biosens. Bioelectron.*, 2012, **35**, 308–312.

46 D. W. Kim, Y. Zhang, K. L. Cooper and A. Wang, In-fiber reflection mode interferometer based on a long-period grating for external refractive-index measurement, *Appl. Opt.*, 2005, **44**, 5368–5373.

47 Henkel Adhesives, Medical Device Adhesives (http://na.henkel-adhesives.com/medical-device-adhesives-17800.htm), accessed 27 September 2017.

48 A. B. Shreiner, J. Y. Kao and V. B. Young, The gut microbiome in health and in disease, *Curr. Opin. Gastroenterol.*, 2015, **31**, 69–75.

49 G. H. Bowden and Y. H. Li, Nutritional influences on biofilm development, *Adv. Dent. Res.*, 1997, **11**, 81–99.

50 B. W. Holloway, Genetic recombination in Pseudomonas aeruginosa, *J. Gen. Microbiol.*, 1955, **13**, 572–581.

51 K. L. Palmer, L. M. Aye and M. Whiteley, Nutritional cues control *Pseudomonas aeruginosa*, multicellular behaviour in cystic fibrosis sputum, *J. Bacteriol.*, 2007, **189**, 8079–8087.

52 P. Hinterdorfer and A. van Oijen, *Handbook of Single-Molecule Biophysics*, Springer, New York, 2009.

53 B. P. Pal, *Fundamentals of Fibre Optics in Telecommunication and Sensor Systems*, New Age International Publishers, New Delhi, 1992.

54 A. Luo, K. Gao, F. Liu, R. Qu and Z. Fang, Evanescent-field coupling based on long period grating and tapered fiber, *Opt. Commun.*, 2004, **240**, 69–73.

55 J. F. Ding, A. P. Zhang, L. Y. Shao, J. H. Yan and S. He, Fiber-taper seeded long-period grating pair as a highly sensitive refractive-index sensor, *IEEE Photonics Technol. Lett.*, 2005, **17**, 1247–1249.

56 Y. Tian, W. Wang, N. Wu, X. Zou and X. Wang, Tapered Optical Fiber Sensor for Label-Free Detection of Biomolecules, *Sensors*, 2011, **11**, 3780–3790.

57 W. D. Bascom, Structure of Silane Adhesion Promoter Films on Glass and Metal Surfaces, *Macromolecules*, 1972, **5**, 792–798.

58 E. P. Plueddemann, Silane adhesion promoter in coatings, *Prog. Org. Coat.*, 1983, **11**, 297–308.

59 O. Sanni, C. Y. Chang, D. G. Anderson, R. Langer, M. C. Davies, *et al.*, Bacterial Attachment to Polymeric

Materials Correlates with Molecular Flexibility and Hydrophilicity, *Adv. Healthcare Mater.*, 2015, **4**, 695–701.

60 N. Jeffery, K. Kalenderski, J. Dubern, A. Lomiteng, M. Dragova, *et al.*, A new bacterial resistant polymer catheter coating to reduce catheter associated urinary tract infection (CAUTI): A first-in-man pilot study, *Eur. Urol., Suppl.*, 2019, **18**, e377.

61 M. Fischer, G. J. Triggs and T. F. Krauss, Optical Sensing of Mirobial Life on Surfaces, *Appl. Environ. Microbiol.*, 2015, **82**(5), 1362–1371.

62 C. T. Nguyen, W. Jung, J. Kim, E. J. Chaney, M. Novak, *et al.*, Noninvasive in vivo optical detection of biofilm in the human middle ear, *Proc. Natl. Acad. Sci. U. S. A.*, 2012, **109**(24), 9529–9534.

63 R. Kashyap and G. Nemova, Surface Plasmon Resonance-Based Fiber and Planar Waveguide Sensors, *J. Sens.*, 2009, 1687–1725.

64 P. Y. Liu, L. K. Chin, W. Ser, H. F. Chen, C. M. Hsieh, *et al.*, Cell refractive index for cell biology and disease diagnosis: *past*, *present* and *future*, *Lab Chip*, 2016, **16**, 634–644.